5-9-2017

Validation of a Method to Estimate Skin Spectral Reflectance Using a Digital Camera.

Christopher Thorstenson
ct4609@rit.edu

R·I·T

Validation of a Method to Estimate Skin Spectral Reflectance Using a Digital Camera.

by

Christopher Thorstenson

A Thesis Submitted in Partial Fulfillment of the
Requirements for the Degree of Masters of Science
in Color Science

Program of Color Science
College of Science
Rochester Institute of Technology
Rochester, NY

May 9, 2017

Signature of Author _____

Accepted by _____
Dr. Mark Fairchild, Graduate Program Director Date

COLLEGE OF SCIENCE

ROCHESTER INSTITUTE OF TECHNOLOGY

ROCHESTER, NEW YORK

CERTIFICATE OF APPROVAL

MASTERS DEGREE THESIS

The Masters Degree Thesis of Christopher Thorstenson

Has been examined and approved by the

Committee as satisfactory for the

Thesis required for the

Masters degree in Color Science

_____

Dr. Mark D. Fairchild, Advisor

_____

Dr. Michael Murdoch

_____

Date

THESIS RELEASE PERMISSION

ROCHESTER INSTITUTE OF TECHNOLOGY

PROGRAM OF COLOR SCIENCE

Title of Thesis:

Validation of a Method to Estimate Skin Spectral Reflectance Using a Digital Camera.

I, Christopher Thorstenson, hereby grant permission to Wallace Memorial Library of R.I.T. to reproduce my thesis in whole or in part. Any reproduction will not be for commercial use or profit.

Signature _____

Date

Abstract

The accurate measurement of skin color and skin spectral reflectance is becoming increasingly desirable due to its application across several domains, including medical, cosmetics, graphic arts, automation, and social science fields. While there exist robust ways to accurately measure color and spectral reflectance, these methods typically require the use of specialized instruments which are often expensive, invasive, and require expert training. Therefore, it would clearly be advantageous to develop methods that can extract accurate colorimetric and spectral data from readily-available, inexpensive digital RGB cameras. Such methodology involves overcoming several fundamental obstacles due to the limitations of RGB camera data.

The current paper reviews the importance of accurate skin color and skin spectral reflectance to several domains. The paper continues by describing an existing methodology (i.e., ColourWorker) that overcomes the limitations inherent in using RGB camera data to estimate spectral reflectance. Finally, the paper presents two experiments that test the validity of ColourWorker in estimating skin spectral reflectance. Experiment 1 compares the ground-truth skin spectral reflectance data obtained from a spectroradiometer (taken from the face of volunteers at rest) to spectral reflectance data estimated from an RGB camera using ColourWorker. Experiment 2 compares the ground-truth skin spectral reflectance data obtained from a spectroradiometer (taken from the hand of volunteers with changing physiological states) to spectral reflectance data estimated from an RGB camera using ColourWorker. The results show good performance in ColourWorker's ability to estimate skin spectral reflectance, and suggest that performance can be improved with careful consideration of reference spectra.

Acknowledgements

I would like to thank my advisor, Dr. Mark Fairchild, for his guidance, advice, and patience throughout this process. It has been a pleasure to work and learn with him over the past years.

I would like to thank my family, Romina, Jeff, and Jillian, who have been unending in their support. I would not be where I am without them.

I would like to thank my RIT cohort, Ben Bodner, Nargess Hassani, and Yixuan Wang. I could not imagine navigating the program without our collaborative efforts. I would also like to thank fellow students, especially Brittany Cox, Joel Witwer, Dr. Yuta Asano, Dr. Max Derhak, Dr. Jennifer Kruschwitz, Dr. Adrià Forés Herranz, and Dr. David Long, for their advice and support throughout the program.

I would like to thank Dr. Roy Berns, Dr. Susan Farnand, Dr. David Wyble, and Dr. Michael Murdoch, for sharing their knowledge and time with me over these past few years.

I would like to thank Valerie Hemink for her constant help and encouragement.

I would like to thank my UR advisor, Dr. Andrew Elliot, for supporting my autonomy in pursuing this program.

Finally, I would like to thank Dr. John Anderson for providing a considerable amount of time and help in working with me on the ColourWorker functionality.

Contents

List of Figures

List of Tables

1. Introduction

The accurate measurement of skin color is increasingly gaining importance due to its useful applications across several domains. The assessment of skin color is valuable to medical fields (e.g., identifying cutaneous or cardiovascular illnesses such as diabetes, cyanosis, and hypertension; Changizi & Rio, 2010), the cosmetics industry (e.g., skin tone matching; Kikuchi, Masuda, & Hirao, 2013), graphic arts (e.g., skin modeling and portraiture; Sun & Fairchild, 2002), and skin color segmentation for automated face processing (e.g., detection and recognition; Hsu, 2002; Yip & Sinha, 2002). Additionally, skin color has become increasingly studied in social sciences. For instance, recent research has shown that skin color can indicate aerobic fitness (Johnson, 1998), presence of sex hormones (Charkoudian, Stephens, Pirkle, Kosiba, & Johnson, 1999), ovulatory cycle in women (Burriss et al., 2015), and emotional responses (Drummond, 1994), and that facial color can influence perceptions of health (Stephen, Law Smith, Stirrat, & Perrett, 2009), attractiveness (Re, Whitehead, Xiao, & Perrett, 2011), emotion (Young, Thorstenson, & Pazda, 2016), and personality (Stephen, Oldham, Perrett, & Barton, 2012). It is clear from this that colorimetric measurement of skin provides useful computational, medical, aesthetic, and social information.

The spectral reflectance of skin (i.e., the proportion of light reflected by skin as a function of wavelength) provides additional information that colorimetric values cannot. For instance, skin spectral reflectance data is necessary to model skin appearance under varying illumination conditions (e.g., from natural daylight to

artificial lighting). Further, skin spectral reflectance can be used to extract information about skin chromophores (e.g., melanin, hemoglobin concentration, and hemoglobin oxygenation; Nishidate, Aizu, & Mishina, 2004), which are important physiological parameters that can be used to predict health, emotion, and skin type. Therefore, the accurate measurement of skin reflectance, as well as skin color, is valuable to several fields, including medical, cosmetic, aesthetic, and visual and social research.

2. Background

2.1. Remote Measurement of Color

There currently exist several instruments that accurately measure colorimetric and reflectance data from objects (e.g., spectrophotometers, spectral radiometers). However, such devices are highly specialized (requiring advanced training to operate), cost prohibitive, and sometimes invasive (requiring device-to-surface contact). Given the availability and low cost of regular commercial RGB cameras, it would seem ideal to explore methodology that involves measurement (or estimation) of spectral reflectance and colorimetric data using readily-available RGB cameras.

Color is difficult to measure accurately with a camera, due to a range of issues. First, cameras represent color using three distinct numbers relating to the three detectors (RGB). However, because reflectance spectra vary continuously as a function of wavelength, cameras only offer an incomplete representation of the

available color information. Additionally, illumination can vary across scenes, which affects the intensity of light reflected from objects.

Despite these limitations, past research has shown that color information from RGB cameras can be extracted and used to reconstruct reflectance spectra using various techniques. These typically involve either the use of multiple chromatic filters with known spectral characteristics (Imai & Berns, 1999), or characterizing the camera sensitivities and modeling spectral estimates based on reference spectra (Chiao, Osorio, Vorobyev, & Cronin, 2000; Zhang et al., 2017).

For instance, Imai and Berns (1999) demonstrated that the spectral reflectance data of paintings can be recovered by combing a conventional RGB camera with either a set of chromatic absorption filters (specifically, a blue, green, and no filter) or multiple lighting sources (specifically Illuminants A and D65). This technique takes advantage of the fact that pigments used in paintings contain predictable spectral curves, minimizing the degrees of freedom needed to estimate them, and then determines the relationship between the camera's digital counts and variation due to changes in either the multiple filters or multiple lighting conditions. The researchers found that a linear method could be applied to estimate the spectral reflectance from the camera's digital counts for their test patches. The limitation of this method is that it requires the target to remain fixed across multiple measurements, while cycling through either multiple absorption filters or multiple lighting conditions.

An alternative method involves characterizing the camera sensitivities and modeling spectral estimates based on reference spectra (Chiao et al., 2000; Zhang et

al., 2017). The current research aims to test the validity of skin spectral estimation using this latter method (reviewed below). Specifically, the current project tests the ability of an existing system (i.e., ColourWorker; Anderson, Hallam, Nduka, & Osorio, 2015) to reliably estimate skin reflectance.

2.2. ColourWorker Functionality

As mentioned previously, reconstructing spectral measurements from RGB cameras presents at least two main problems. First, illumination conditions (i.e., a range of natural and artificial sources, such as daylight vs. fluorescent lighting) under which camera recordings take place can vary across scenes. ColourWorker deals with this problem by incorporating a calibration standard (e.g., X-rite ColorChecker) with known reflectance spectra. The calibration standard is used to estimate the camera (RGB) responses as a function of wavelength relative to a white reference. Because the spectral characteristics of the calibration standard are known, this procedure allows an estimation of the camera model and the illumination conditions. The camera model is estimated by iteratively adjusting a set of parameters (spectral sensitivity functions, and intensity response functions) in order to minimize the difference between a measured camera response to the calibration standard and the estimated response predicted by the camera model using a standard least squares approach.

The second main problem is that camera images comprise three specific values (RGB), while reflectance spectra vary continuously as a function of wavelength. This is a problem because any given RGB signal can be reproduced by an infinite number of reflectance spectra. ColourWorker deals with this problem by

taking advantage of the fact that the reflectance spectra of natural materials (such as skin) vary predictably, and are often influenced by three or fewer variables. Therefore, the system can make use of a set of reference spectra measured from the material of interest (in this case, skin) to estimate the likely reflectance spectra produced given the RGB signal through linear modeling (see Anderson et al., 2015, for more detailed information on this method). The specific reference spectra and measurement details will be discussed in the Methods section for each experiment.

2.3. Basics of Color Vision

The first step in human vision occurs when light reflects or emanates from an object or source, enters the eye, and is imaged on the retina. There, the photoreceptor cells' pigment molecules absorb the light and transduce electrical neural signals. There are two main classes of photoreceptor, rods and cones, which are functionally distinct. Rods operate at low light (scotopic) conditions, while cones operate at higher light (photopic) conditions, with a midrange where both cones and rods operate (mesopic). High resolution and color vision are present under photopic conditions. While rods may have some effect on color perception under mesopic conditions, their influence is small and can be ignored. Humans have three classes of cones. The spectral absorption characteristics of the short (S), medium (M), and long (L) wavelength cones are distinguished by the spectral sensitivities of their visual pigments (see Figure 2-1). Our perception of color relies on having these three types of cones which respond to, and integrate, light at various wavelengths. The integration of these cone responses forms three color-opponent axes (Berns, 2000). The luminance axis (black – white) results from the addition of L- and M- cone

activation. A red-green chromatic axis results from subtracting M-cone activation from L-cone activation. A yellow-blue chromatic axis results from the addition of L- and M- cone activation, and subtracting S-cone activation. The color-opponent signals then leave the retina via the optic nerve for further processing in cortical and subcortical areas of the brain (for a comprehensive review of color vision processes, see Gegenfurtner & Kiper, 2003, and Goldstein et al., 2004).

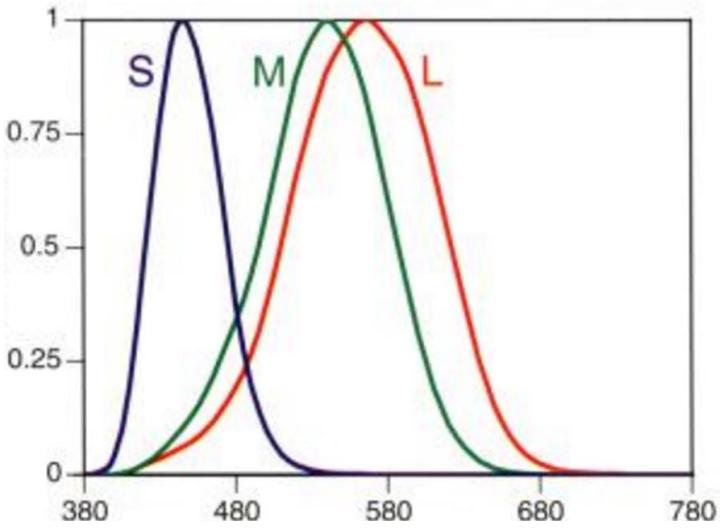

Figure 2-1. Relative spectral sensitivity of the S, M, and L cones by wavelength (from Berns, 2000).

2.4. Skin Properties

Skin reflectance is influenced by various chromophores in the skin that absorb light in different ways. Along the visible range of wavelength, the primary chromophores that influence skin reflectance are hemoglobin and melanin (Zonios, Bykowski, & Kollias, 2001). The absorptive properties of hemoglobin (see Figure 2-2) are responsible for blood's reddish color, which is found in the vascular structures of the dermis, approximately 50-500 μm below the skin surface. Further, oxygenated and deoxygenated hemoglobin have slightly difference absorption spectra;

approximately 90-95% of hemoglobin is oxygenated in the arteries, while only about 47% of the hemoglobin is oxygenated in the veins (Baranoski & Krishnaswamy; 2010).

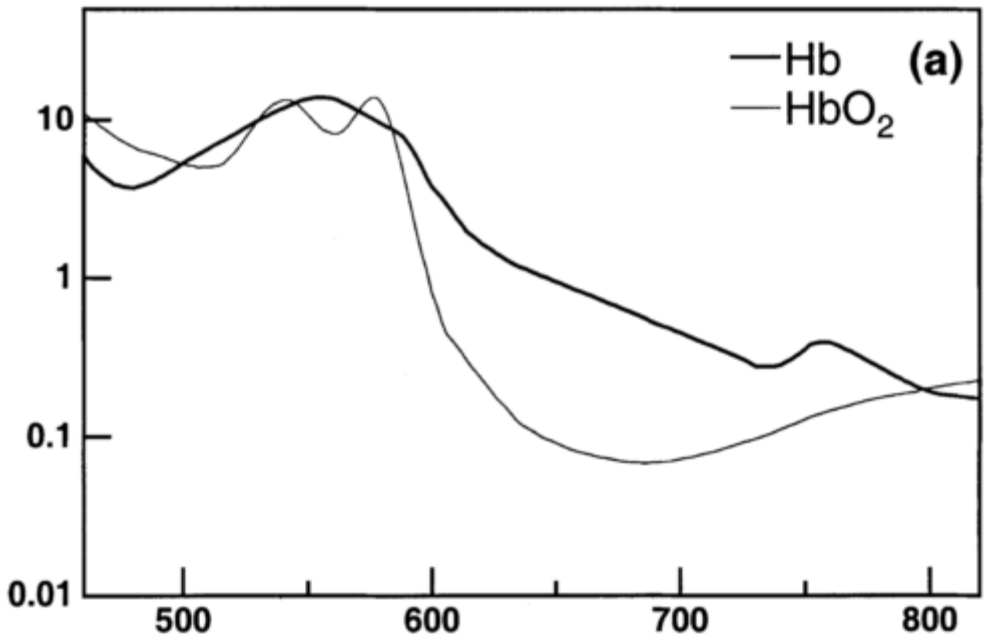

Figure 2-2. Molecular extinction coefficient spectra of oxyhemoglobin and deoxyhemoglobin. From Zonios et al. (2001).

Melanin is found in the epidermis, approximately the top 50-100 μm of the skin. Melanin is largely responsible for the variation in skin color across the human population. The concentration of melanin in human skin ranges from low (Type I; light Caucasian skin) to high (Type VI; black African skin). Additionally, UV radiation provokes temporary increases in melanin concentration. Melanin absorbs light strongly in the ultraviolet and low-visible range (see Figure 2-3), which lends to its photo-protective properties (Zonios et al., 2001).

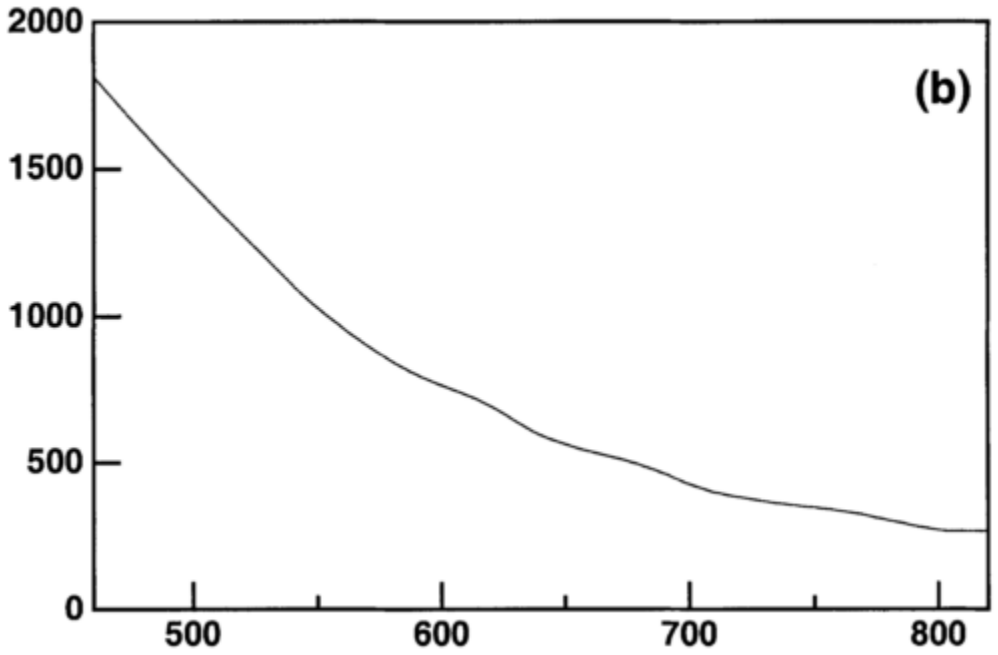

Figure 2-3. Molecular extinction coefficient spectra of melanin. From Zonios et al. (2001).

While melanin concentration is relatively stable over time, Hemoglobin concentration and oxygenation are transient, able to fluctuate significantly over short periods of time. Dilation of the blood vessels, which increases the volume fraction of the blood in the dermis, can be caused by a range of stimulation, including pressure, temperature, vasoactive drugs, and psychological stress (Piérard, 1998).

Changes in hemoglobin concentration and oxygenation is responsible for skin color changes due to dilation of blood vessels. Changes in these two variables lead to predictable changes in the reflectance and color of skin. Skin reflectance in the visible range contains a characteristic 'W' feature (~525-575 nm) due to the absorptive properties of oxygenated hemoglobin. Greater hemoglobin oxygenation leads to a more prominent 'W' feature, increasing L-cone activation relative to the M-cone, resulting in redder skin. Greater hemoglobin concentration in the skin raises the

entire 'W' feature, increasing M- and L-cone activation relative to the S-cone, resulting in bluer skin (see Figure 2-4; Changizi, Zhang, & Shimojo, 2006).

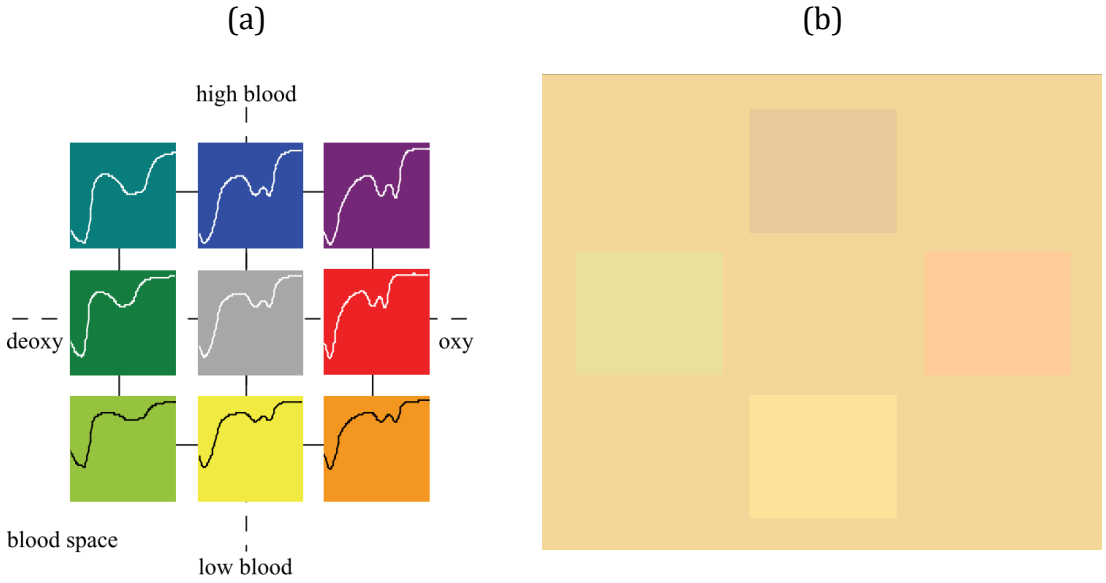

Figure 2-4. Example of skin spectral reflectance (a) and color (b) modulations as a function of hemoglobin properties. From Changizi et al. (2006) and Changizi & Rio (2010).

The purpose of the current research is to test the functionality of the system (ColourWorker) to accurately estimate skin reflectance and colorimetric data from digital video taken from an RGB camera. As discussed previously, the accurate estimation of reflectance and colorimetric data from digital cameras has many applications across several domains (e.g., medical, cosmetic, graphic arts, automated systems, social science). Social science research, in particular, can benefit from inexpensive and non-invasive measurements of skin color and spectral reflectance. For instance, face color has been shown to influence the perception of social

characteristics such as health, attractiveness, emotion, and personality. The accurate color measurement of actual faces can facilitate our understanding of the relationship between skin color and social perception. Further, because skin spectral reflectance can be used to extract physiological variables (e.g., hemoglobin, melanin), we can gain a much richer understanding of the influence of physiology on social perception, guided by skin color. Therefore, Experiment 1 tests whether skin color and spectral reflectance can be accurately estimated from camera RGB data. Finally, because some social states (e.g., emotion) involve transient changes of physiology (e.g., hemoglobin changes), the current research emphasizes measurements of change over time. Therefore, Experiment 2 tests whether changes in skin color and spectral reflectance can be accurately captured from camera RGB data.

In Experiment 1, subjects were video-recorded at rest, while ground-truth measurements were taken from a spectroradiometer. The system provided estimates of skin reflectance and CIELAB color values, which were compared to the ground-truth data. In Experiment 2, subjects were video-recorded (and ground-truth measurements were taken with a spectroradiometer) while a blood-pressure cuff was used to manipulate the hemoglobin concentration and oxygenation of the skin. The system again provided estimates of skin reflectance and CIELAB color values, which were compared to the ground-truth data.

3. Experiment 1

Experiment 1 aimed to demonstrate the ability of ColourWorker (see section 2.2) to reliably estimate the reflectance spectra of human skin. The functionality of

ColourWorker was used to generate estimates of skin reflectance from subjects at rest, which were compared to ground-truth measurements of skin reflectance taken simultaneously.

3.1. Methods

3.1.1. Subjects

Five volunteers (2 male, 3 female; 4 Caucasian, 1 Asian, 1 Middle-Eastern) agreed to be video-recorded for the current experiment.

3.1.2. Apparatus

Subjects were seated in room with no natural lighting, facing a PR655 Spectroradiometer and a Canon 5D Mark III digital camera with 24-105mm lens. D50 fluorescent was used as overhead lighting. The spectroradiometer and camera were situated approximately 25 cm apart, at eye-level to the subject, and had roughly equal measurement distance to the target (approx. 60 cm). A 24-patch X-rite ColorChecker was included the frame in order to estimate the camera model. A halon PRD was included to measure the radiance of the source lighting. A digital timer was included to synchronize video data with spectral measurements. A black cloth was placed in the background to reduce extraneous reflection. See Figure 3-1 for an illustration of the apparatus. See Figure 3-2 for the spectral radiance of the source illuminant. See Figure 3-3 for the spectral reflectance of the ColorChecker patches.

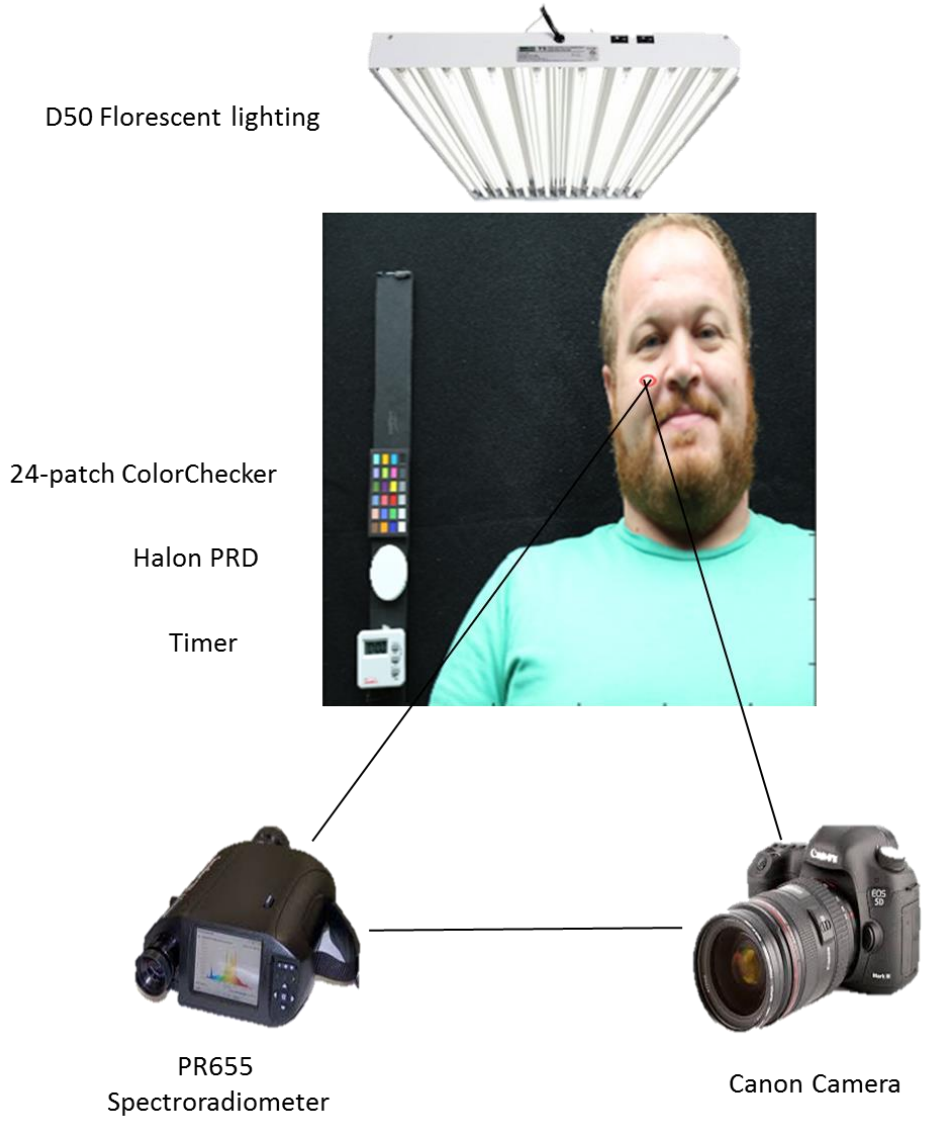

Figure 3-1: Example illustration of the experimental apparatus.

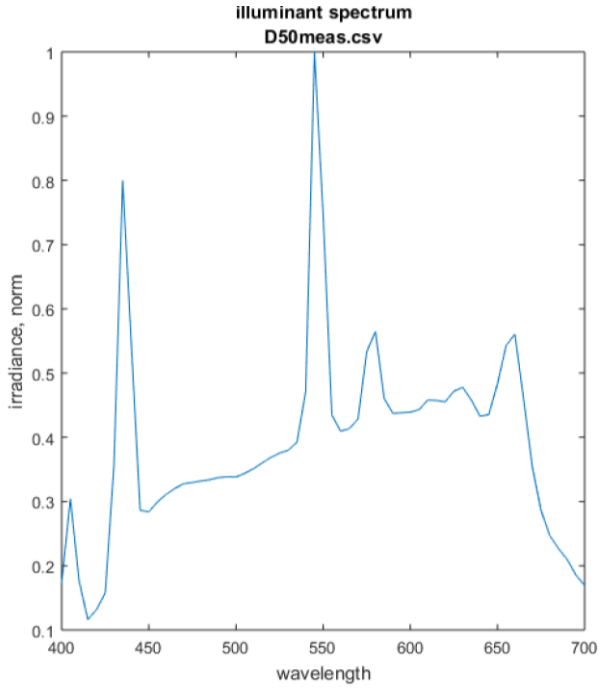

Figure 3-2: Normalized radiance of the source illuminant, measured by a PR655 spectroradiometer.

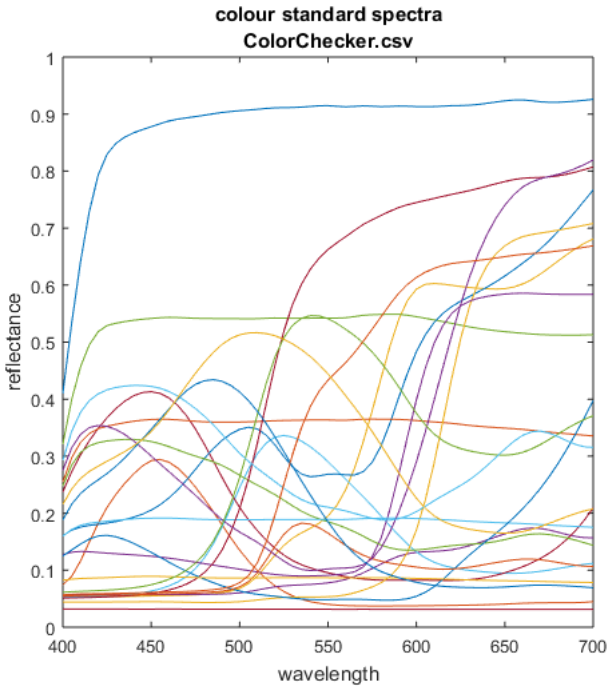

Figure 3-3: Spectral reflectance of the 24-patch ColorChecker measured by an i1-pro spectrophotometer

3.1.3. Procedure

For each session, subjects were told that their faces would be video-recorded. They were instructed to remain still and to breathe regularly during the recording, but were otherwise given no further instructions.

Once the subject was ready to begin, the digital timer was started and the camera began recording at 30 frames per second. While the camera was recording, the experimenter took 4 measurements using the spectroradiometer, each approximately 20 seconds apart. The experimenter recorded the timestamp from the digital timer for each measurement. The video was saved as a MOV file.

3.1.4. Measured Reflectance Spectra

Before recording, the spectroradiometer was focused on the Halon PRD to measure the radiance of the source illuminant. Following this measurement, the spectroradiometer was focused on the subject's cheek for the remainder of the session. Each spectroradiometer measurement provided the radiance of the skin. The spectral reflectance of the skin was derived by dividing the skin measurement by the source measurement.

3.1.5. Estimated reflectance spectra

Still-frames corresponding to the timestamp of each spectroradiometer measurement were read from the camera recording and were saved as TIF files (dimensions 1080 x 1920). The functionality of ColourWorker (see section 2.2) was used to computationally estimate the reflectance spectra of the cheek area for each frame. In some cases, specular highlights in this area caused excessive noise that prevented reliable reflectance estimation, so the sampled location was slightly

adjusted. This method involves two primary steps. First, it accounts for variation in illumination and camera response sensitivities by incorporating the measured reflectance spectra of an in-frame color standard (a 24-patch X-Rite Macbeth ColorChecker). Second, it uses a set of target-relevant reference spectra (in this case, skin reflectance) and linear modeling to estimate the specific spectrum likely to have been produced by the RGB camera signal. The reference spectra used in the current experiment were measured spectral reflectance curves from the back of a human (Caucasian) hand during blanching, caused by applying surface pressure. See Figure 3-4 for the reference spectra used in the current experiment. Additionally, it was found that applying an additive scaling factor of 0.095 slightly improved the fit of the results (This value was derived *post hoc* from the average distance between measured and estimated data in the sample).

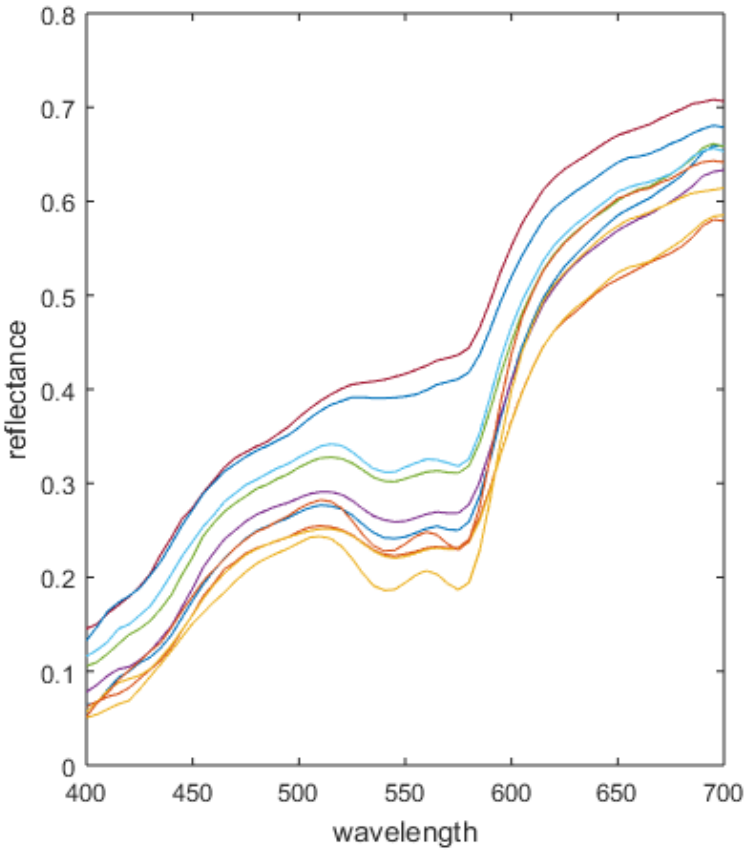

Figure 3-4: Reference spectra used in Experiment 1. Measured spectral reflectance curves from the back of a human hand during blanching caused by applying surface pressure.

3.2. Results and Discussion

3.2.1. Results

For each frame, the cheek area was sampled and a reflectance estimate was created for each pixel in a 10-pixel radius of the sampled area. For each subject, the mean and standard deviation of the estimated reflectance spectra were calculated across the 4 frames sampled during the session (see Figure 3-5). The estimated reflectance spectra data were compared to the mean PR655-measured reflectance data for each subject using Pearson's correlation (r) and root-mean-squared-error (RMSE; see Table 3-1). Additionally, CIELAB L*, a*, and b* values, corresponding to Lightness, redness, and yellowness, respectively, were calculated for measured and estimated data (see Figures 3-6 to 3-8, and Table 3-2).

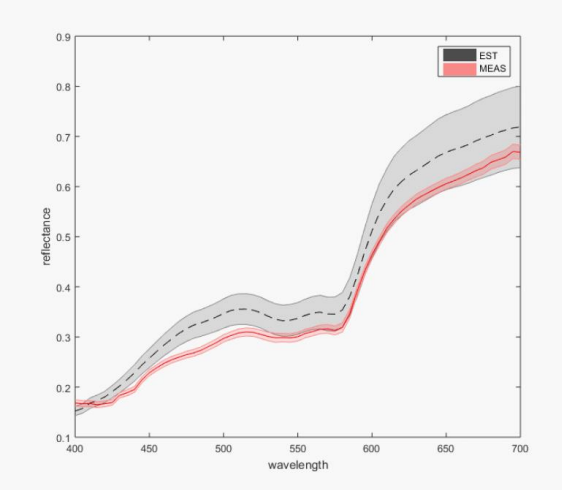

1.1

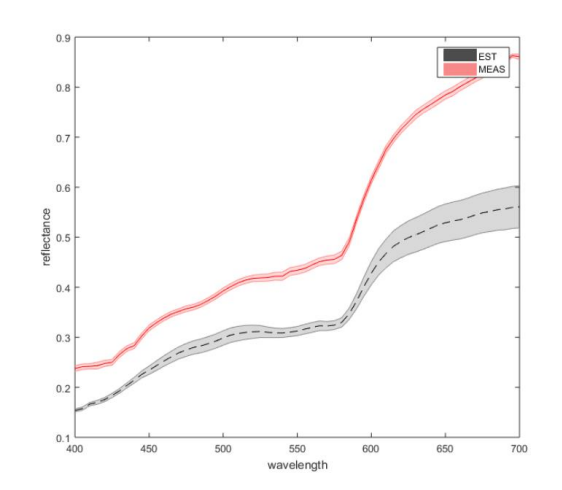

1.2

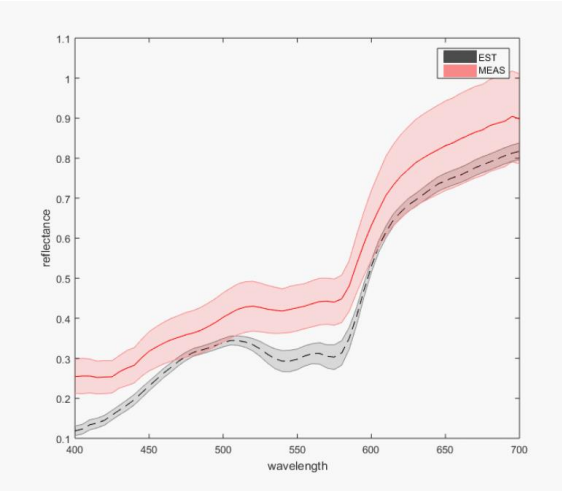

1.3

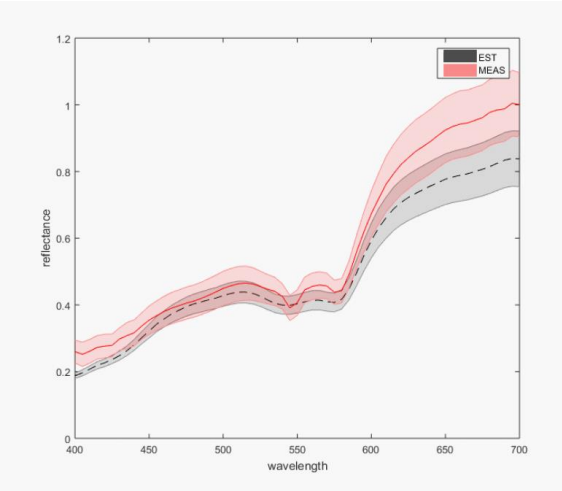

1.4

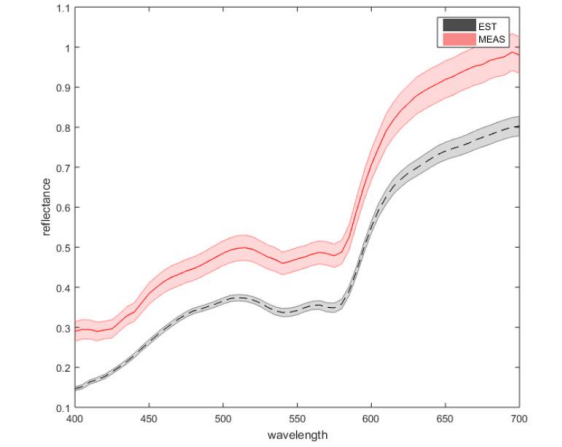

1.5

Figure 3-5: Estimated reflectance spectra (M+/-SD) against Measured reflectance spectra (M+/-SD) for each subject. Subject identifiers below each chart.

Table 3-1: Correlation (r) and root-mean-square-error (RMSE) for each subject's estimated versus measured reflectance.

Subject	*r*	RMSE
1.1	0.9979	0.0419
1.2	0.9962	0.1533
1.3	0.9946	0.0962
1.4	0.9943	0.0684
1.5	0.999	0.1420
Mean	0.9964	0.10036

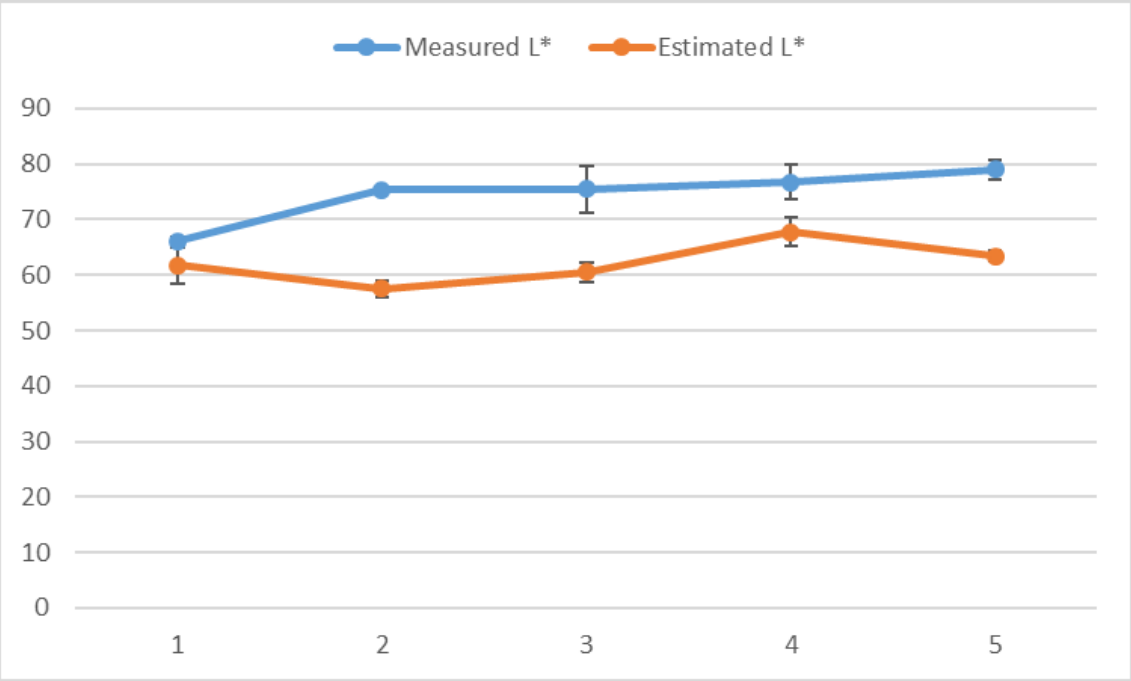

Figure 3-6. Mean+/-SD of L* error between measured and estimated colorimetric data for each of 5 subjects.

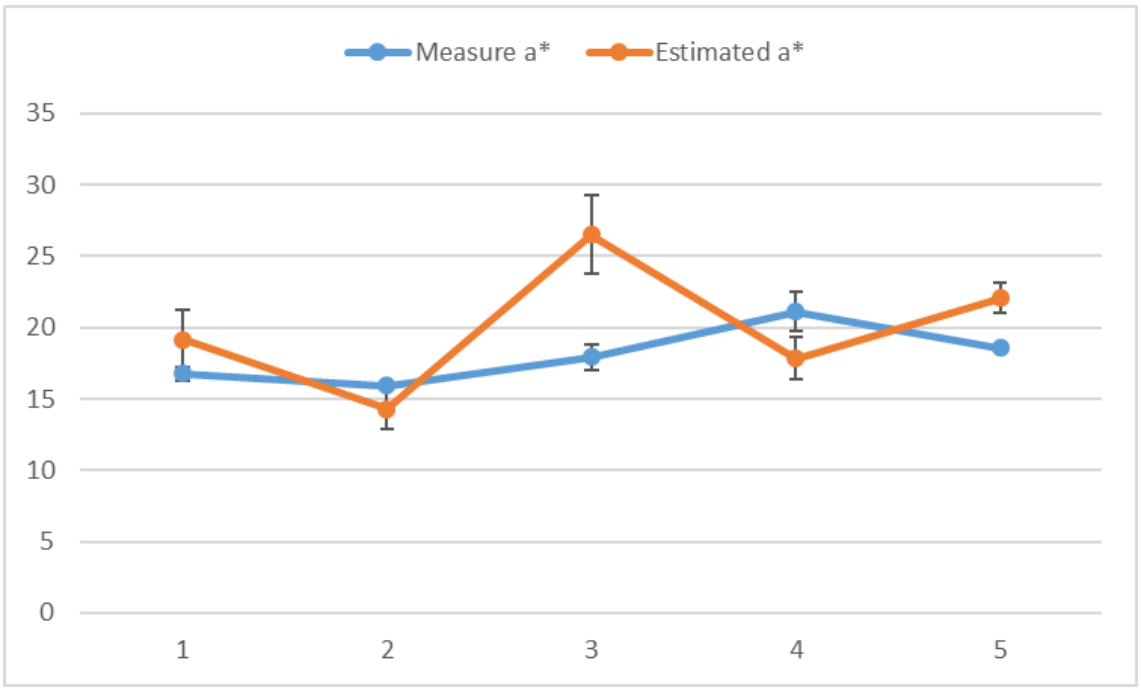

Figure 3-7. Mean+/-SD of a* error between measured and estimated colorimetric data for each of 5 subjects.

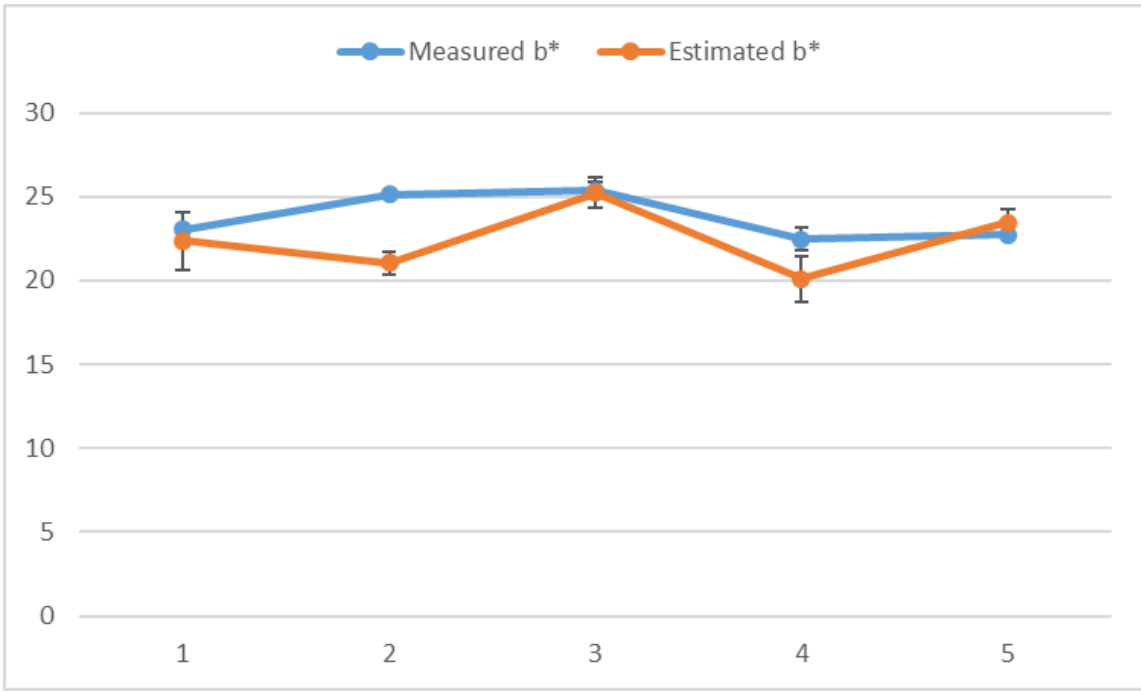

Figure 3-8. Mean+/-SD of b* error between measured and estimated colorimetric data for each of 5 subjects.

Table 3-2. CIELAB values for each subject's estimated versus measured colorimetric data.

Subject	L*meas	L*est	a*meas	a*est	b*meas	b*est	Δ L*	Δ a*	Δ b*	Δ E*
1.1	66.09	61.73	16.76	19.17	23.05	22.35	4.36	2.41	0.71	5.03
1.2	75.40	57.48	15.95	14.29	25.13	21.04	17.93	1.66	4.09	18.47
1.3	75.45	60.54	17.94	26.52	25.38	25.22	14.91	8.57	0.16	17.20
1.4	76.73	67.75	21.11	17.85	22.47	20.08	8.98	3.26	2.39	9.85
1.5	78.97	63.42	18.57	22.07	22.72	23.45	15.55	3.50	0.73	15.96
Mean							**12.35**	**3.88**	**1.62**	**13.05**

3.2.2 Discussion

The results revealed some inconsistency between the estimated and measured reflectance spectra. The most obvious source of error is in the scaling of the estimated data. This error was attenuated by uniformly applying an additive scaling factor to the data (0.095), but a large scaling difference was still evident (see Table 3-1; RMSE = .10). This difference was also evident in the comparison between estimated and measured CIELAB L* values (See Table 3-2; $\Delta L^*_{mean} = 12.35$). However, the estimation of the reflectance curve shape performed better (see Table 3-1; r = .996), as did the estimation of CIELAB a* and b* values (See Table 3-2; $\Delta a^*_{mean} = 3.88$; $\Delta b^*_{mean} = 1.62$).

A potential and likely source of error was the set of reference spectra used. Since the linear modeling involved in the functionality of ColourWorker involves constraining the estimated reflectance to match the patterns of the reference spectra, it is clear that the choice of input reference spectra is critical to estimate variation in observed reflectance spectra. The reference spectra used in the current experiment were generated by applying pressure to the skin and measuring the resulting spectra due to changes in hemoglobin properties under the skin site. However, skin reflectance is largely influenced by melanin content as well as hemoglobin. Further, the current subjects varied in ethnicity, which implies variation in skin type due

primarily to differences in melanin content. Therefore, it is reasonable to assume that estimates of skin reflectance for the current sample could be improved by instead utilizing reference spectra that incorporate changes in melanin content.

4. Experiment 2

Experiment 2 aimed to demonstrate the ability of ColourWorker to reliably estimate changes in the reflectance spectra of human skin that are due to changes in blood flow. The functionality of ColourWorker was used to generate estimates of skin reflectance from subjects at three physiological events related to changes in blood flow: baseline, occlusion, and hyperaemia. These estimates were compared to ground-truth measurements of skin reflectance taken simultaneously.

4.1. Methods

4.1.1. Subjects

Six additional volunteers (3 male, 3 female; Caucasian) agreed to be video-recorded for the current experiment.

4.1.2. Apparatus

Subjects were seated in a room with no natural lighting, and placed their hand face-down on a flat table. The same PR655 Spectroradiometer and Canon camera were used in the current experiment. D50 fluorescent lighting was used as overhead lighting. The spectroradiometer and camera were situated approximately 25 cm apart, approximately 40 cm above the subject's hand, and had roughly equal measurement distance to the target (approx. 40 cm). A 24-patch X-rite ColorChecker was included the frame in order to estimate the camera model. A halon PRD was

included to measure the radiance of the source lighting. A digital timer was included to synchronize video data with spectral measurements. A black board was placed on the table top to reduce extraneous reflection. See Figure 4-1 for an illustration of the apparatus. The spectral reflectance of the ColorChecker patches and spectral radiance of the illuminant were the same as in Experiment 1. To manipulate the blood flow to the arm, a standard manual blood pressure cuff (not in frame) was used.

Figure 4-1: Example illustration of the experimental apparatus in Experiment 2.

4.1.3. Procedure

For each session, subjects were told that their hands would be video-recorded. They were instructed to remain still and to breathe regularly during the recording. Additionally, they were briefed on how the blood pressure cuff would be used. Prior to recording, the subject's systolic blood pressure was measured from the arm of the subject (that was not recorded). After this measurement, the subject was informed that the cuff would be inflated for approximately 4 minutes during the course of the recording, in order to temporarily occlude blood flow to the hand. The subject was told that they would have full control over the cuff's manual air-release valve after the cuff was inflated, so that they could release the pressure in the event that the occlusion became uncomfortable. The subject was then shown how the cuff and release valve worked. No subject felt it necessary to use the valve during the experiment, and none reported more than minor discomfort.

Once the subject was ready to begin, the digital timer was started and the camera began recording at 30 frames per second. The blood pressure cuff was used to alter the blood flow to the subject's arm, using a method similar to Zonios et al., (2001). After approximately 10 seconds, the blood pressure cuff was inflated to a pressure 50 mmHg higher than the subject's resting systolic arterial pressure. This pressure was maintained for 4 minutes in order to occlude blood flow to the hand. After 4 minutes, the pressure was released. While the camera was recording, the experimenter took 3 measurements using the spectroradiometer, corresponding to three specific physiological events: baseline (at approx. 5s), occlusion (at approx. 240s), and hyperaemia (at approx. 260s). See Figure 4-2 for an illustration of the

hemodynamics involved during the time course of the experiment. The experimenter recorded the timestamp from the digital timer for each measurement. The video was saved as a MOV file.

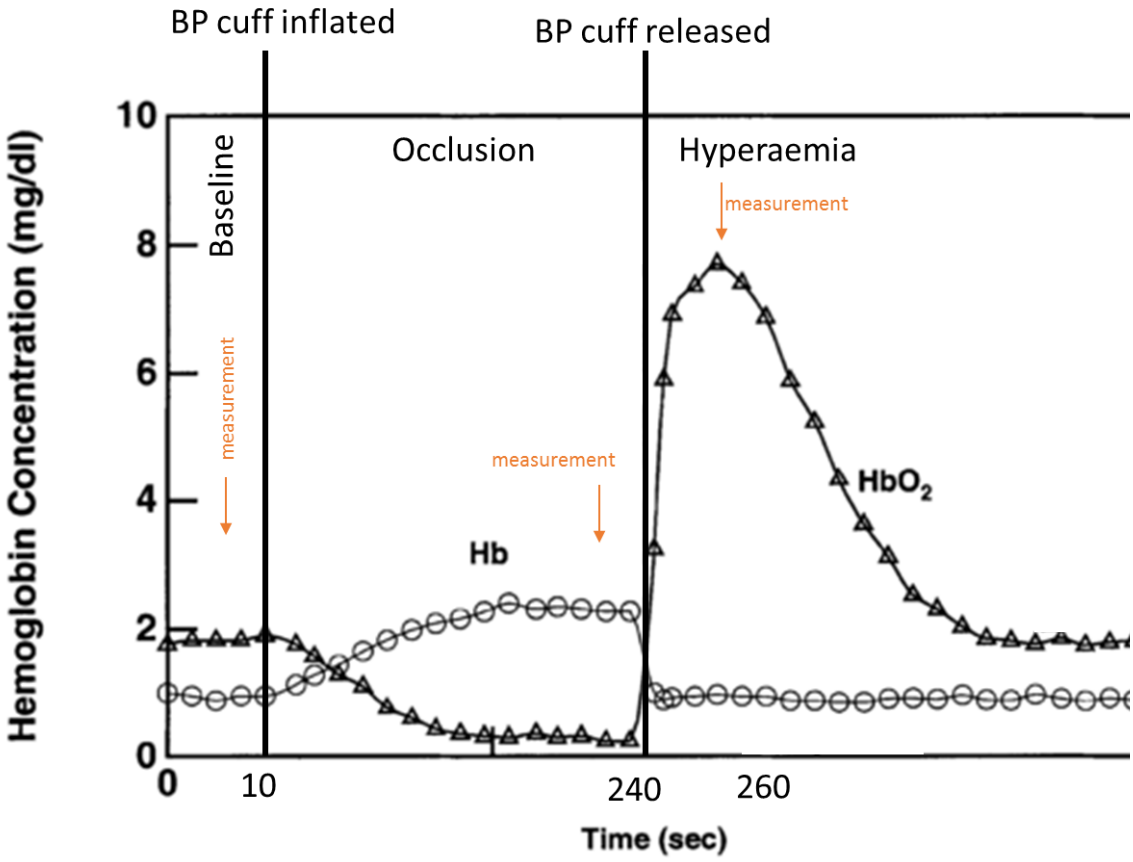

Figure 4-2: Illustration of the hemodynamics involved during the time course of the experiment (adapted from Zonios et al., 2001). The graph represents the concentrations of oxyhemoglobin (Hb02) and deoxyhemoglobin (Hb) in the skin over time. One baseline measurement is taken (5 s) before the blood pressure cuff is inflated. Following the baseline measurement, the cuff is inflated to occlude blood flow to the hand, resulting in an increase in Hb and a concomitant decrease in Hb02. A second measurement is taken at the end of the occlusion period (240 s). Following, the cuff pressure is released, resulting in a rapid influx of oxygenated blood (i.e., hyperaemia). The third measurement is taken during the hyperaemia phase (260 s).

4.1.4. Measured Reflectance Spectra

Before recording, the spectroradiometer was focused on the Halon PRD to measure the radiance of the source illuminant. Following this measurement, the spectroradiometer was focused on the back of the subject's hand (between the thumb and first finger) for the remainder of the session. The measurements were made at the time points described above. Each spectroradiometer measurement provided the radiance of the skin. The spectral reflectance of the skin was derived by dividing the skin measurement from the source measurement.

4.1.5. Estimated Reflectance Spectra

Still-frames corresponding to the timestamp of each spectroradiometer measurement were read from the camera recording and were saved as TIF files (dimensions 1080 x 1920). The functionality of ColourWorker (see section 2.2) was used to computationally estimate the reflectance spectra of the skin area for each frame, in a similar way as in Experiment 1. In some cases, specular highlights in this area caused excessive noise that prevented reliable reflectance estimation, so the sampled location was slightly adjusted. However, for this experiment, a different set of reference spectra, which reflected the dynamic changes in skin blood flow over time, were used. The reference spectra used in the current experiment were the average measured spectral reflectance curves from the back of 3 human (Caucasian) hands undergoing the same blood pressure cuff manipulation as described above. See Figure 4-3 for the reference spectra used in the current experiment.

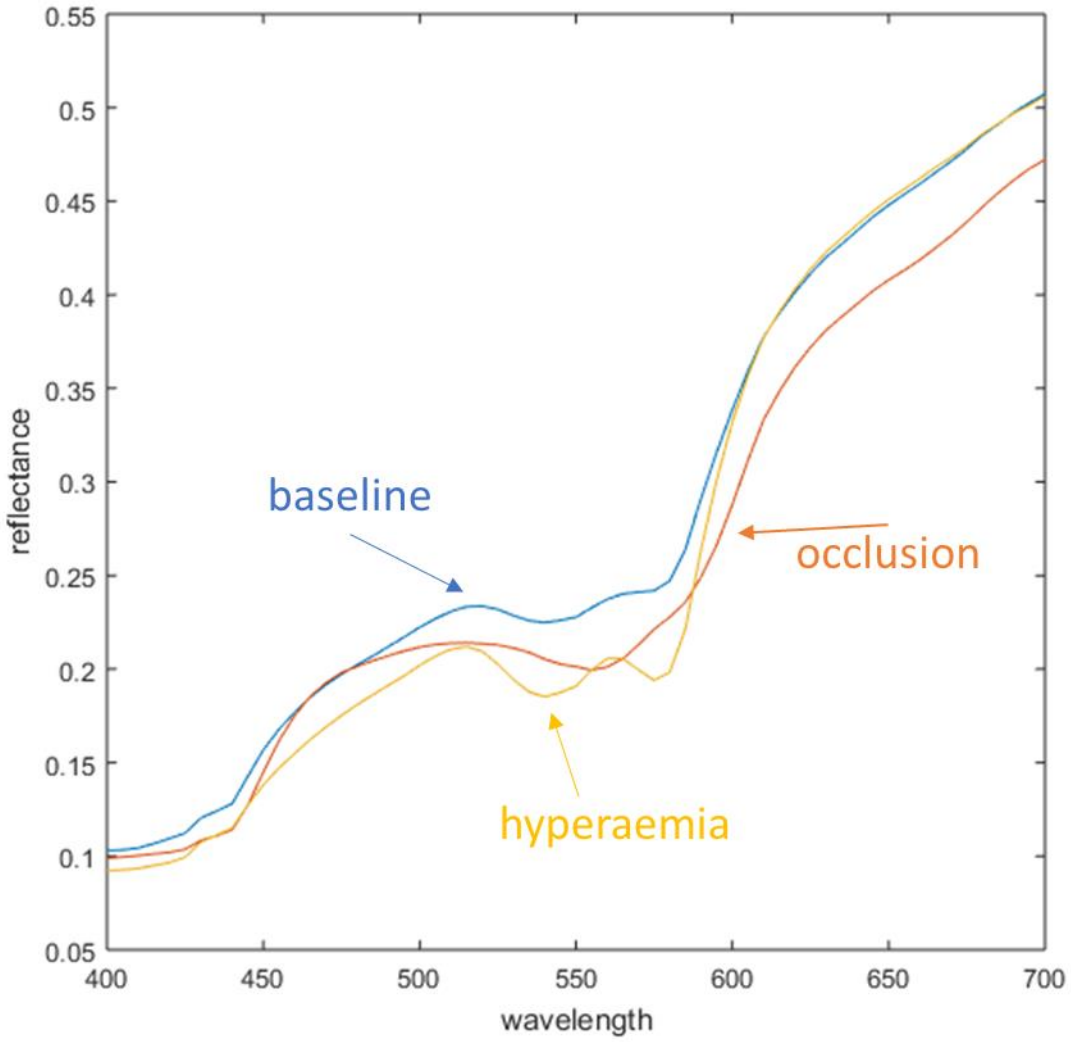

Figure 4-3: Reference spectra used in Experiment 2. Average measured spectral reflectance curves from the back of 3 human hands taken during the baseline, occlusion, and hyperaemia periods of the blood pressure cuff manipulation. The characteristic 'W' shape of skin reflectance (~525-575 nm), which is due to the absorption properties of oxyhemoglobin in this range, is noticeable during baseline. The 'W' shape is lost during occlusion (because of the decrease of oxyhemoblin), but is accentuated during hyperaemia (because of the substantial increase of oxyhemoglobin).

4.2. Results and Discussion

4.2.1. Results

For each frame, the back of the hand was sampled and a reflectance estimate was created for each pixel in a 10-pixel radius of the sampled area. The mean and standard deviation of the estimated reflectance spectra were calculated for each of the frames corresponding to the 3 physiological states sampled during the session (see Figures 4-4 to 4-6). The estimated reflectance spectra data were compared to the mean and standard deviation of the PR655-measured reflectance data for each subject using Pearson's correlation (r) and root-mean-squared-error (see Table 4-1). Additionally, CIELAB L*, a*, and b* values, corresponding to Lightness, redness, and yellowness, respectively, were calculated for measured and estimated data (see Table 4-2, Figures 4-7 to 4-9). Finally, because the current experiment was primarily interested in the estimation of skin color changes over time, CIELAB ΔL*, Δa* and Δb* values (reflecting changes in skin color across physiological states) were calculated and compared between estimated and measured data (see Table 4-3, Figure 4-10).

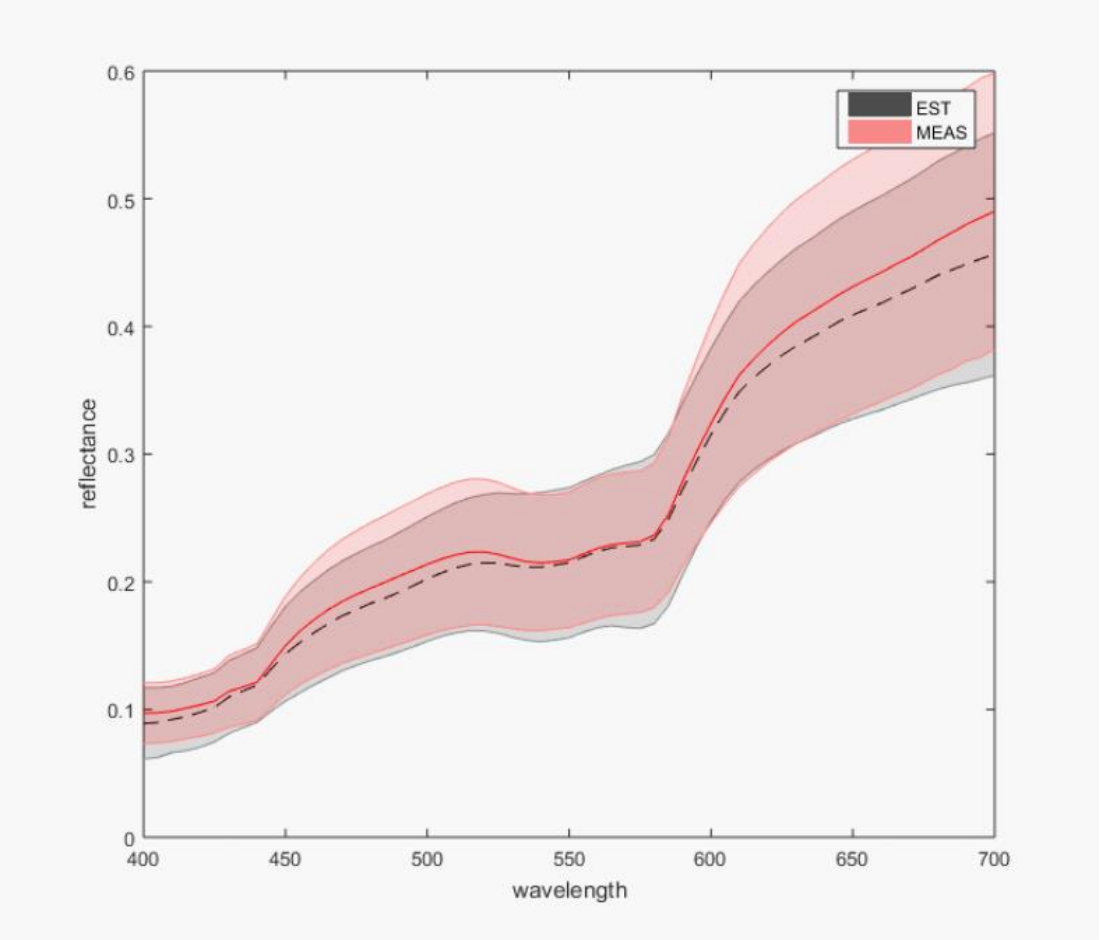

Figure 4-4: Estimated reflectance spectra (M+/-SD) against Measured reflectance spectra (M+/-SD) for all subjects during baseline measurement. For both measured and estimated reflectance spectra, the characteristic 'W' shape of skin reflectance (~525-575 nm), which is due to the absorption properties of oxyhemoglobin in this range, is noticeable during baseline.

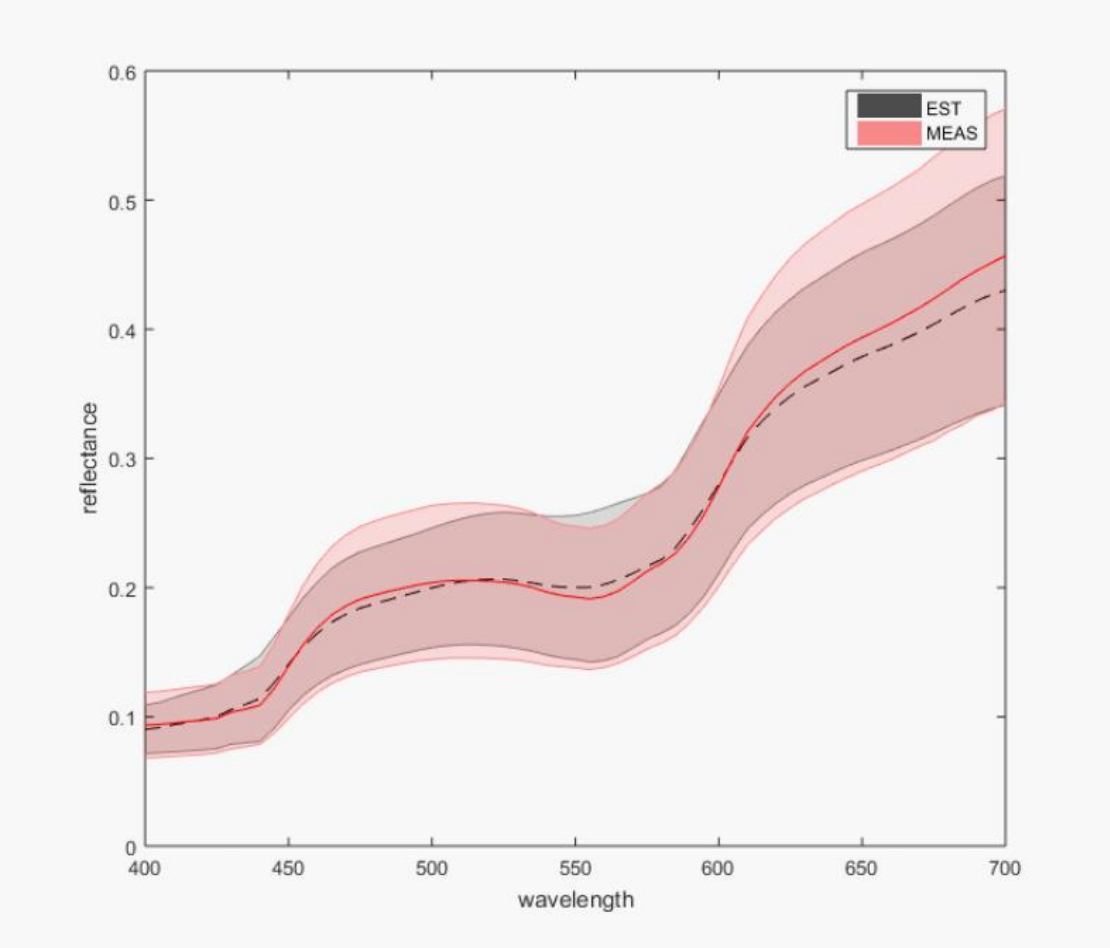

Figure 4-5: Estimated reflectance spectra (M+/-SD) against Measured reflectance spectra (M+/-SD) for all subjects during occlusion measurement. For both measured and estimated reflectance spectra, the 'W' shape is lost during occlusion because of the decrease of oxyhemoblin.

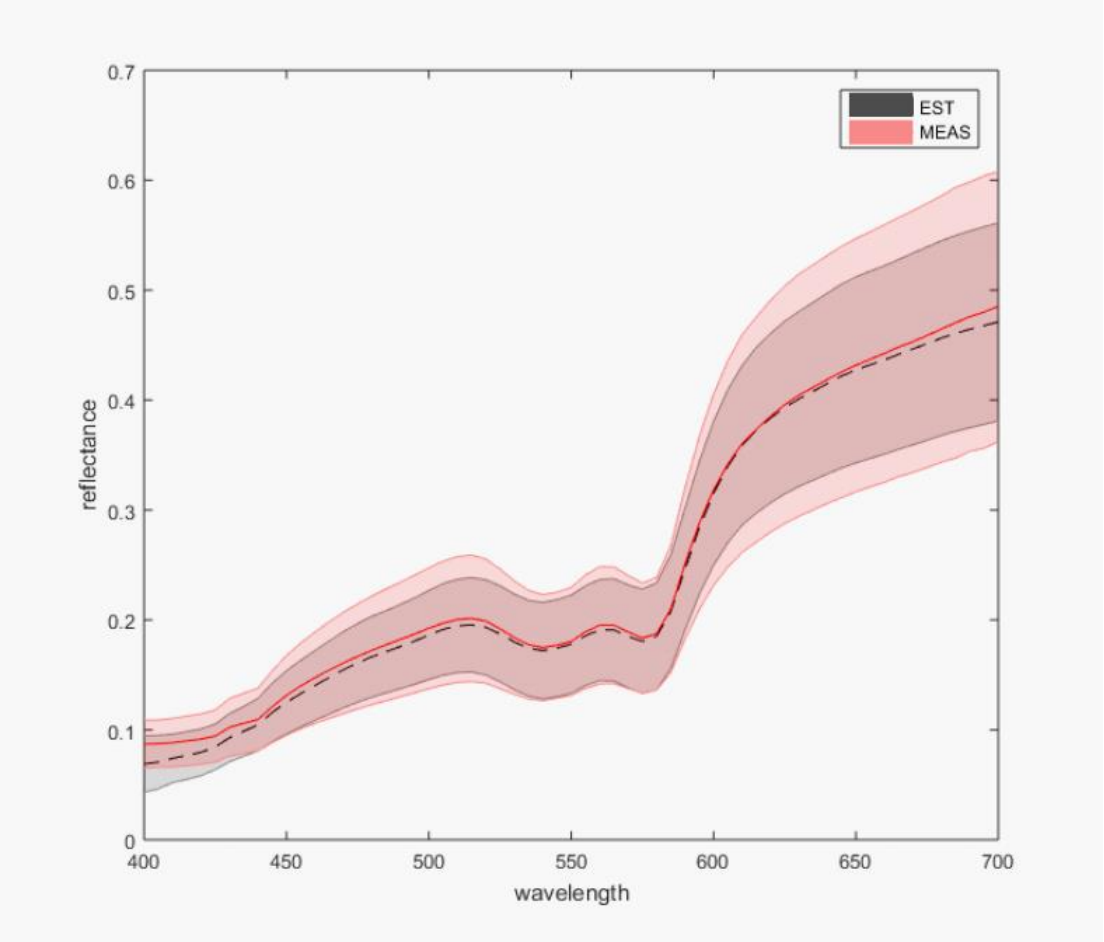

Figure 4-6: Estimated reflectance spectra (M+/-SD) against Measured reflectance spectra (M+/-SD) for all subjects during hyperaemia measurement. For both measured and estimated reflectance spectra, the 'W' shape is accentuated during hyperaemia because of the substantial increase of oxyhemoglobin.

Table 4-1: Correlation (r) and root-mean-square-error (RMSE) for the estimated versus measured reflectance at each physiological state.

	r	RMSE
Baseline	0.9992	0.012
Occlusion	0.9986	0.004
Hyperaemia	0.9996	0.006
Mean	0.9991	0.007

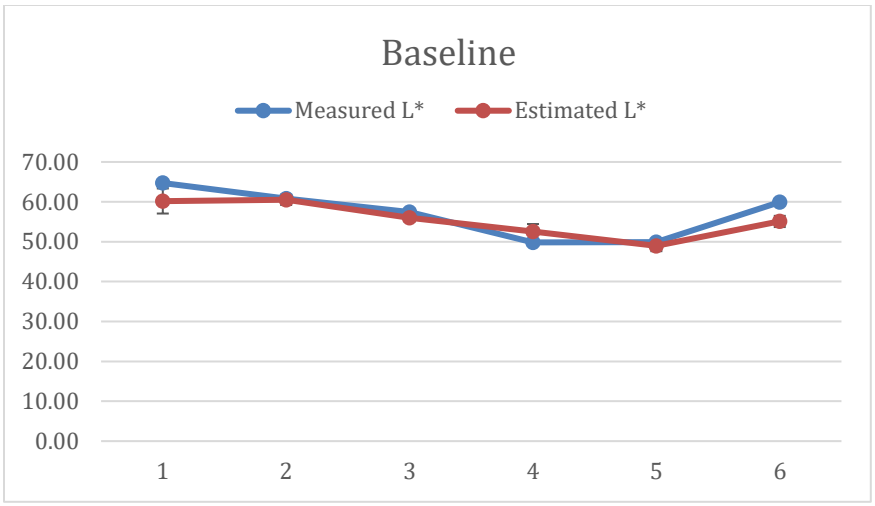

CIELAB L*

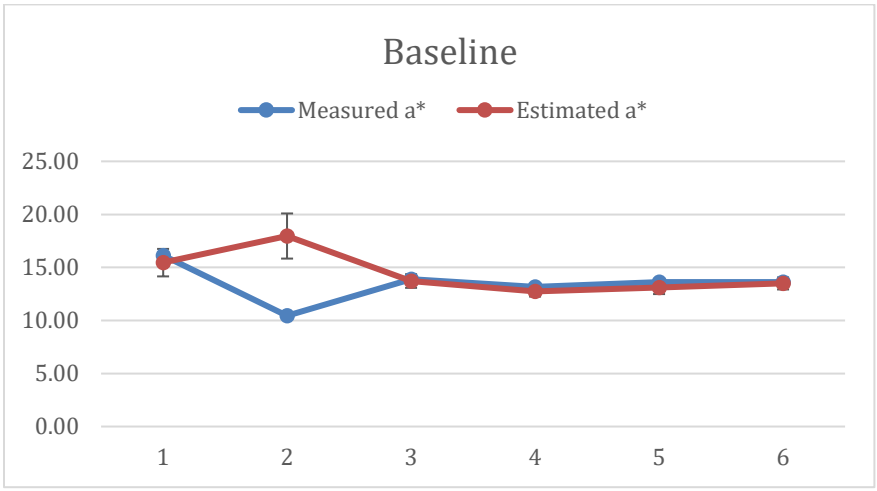

CIELAB a*

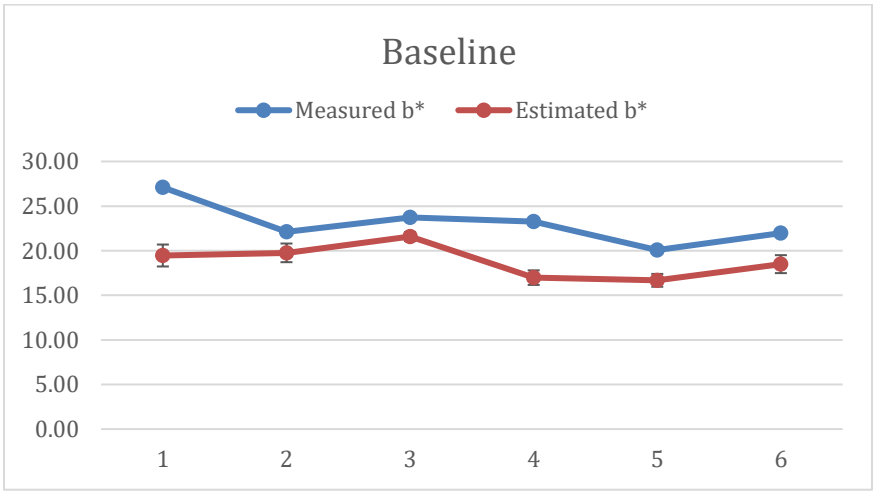

CIELAB b*

Figure 4-7: Mean+/-SD of CIELAB values. Difference between measured and estimated colorimetric data for each of 6 subjects at baseline.

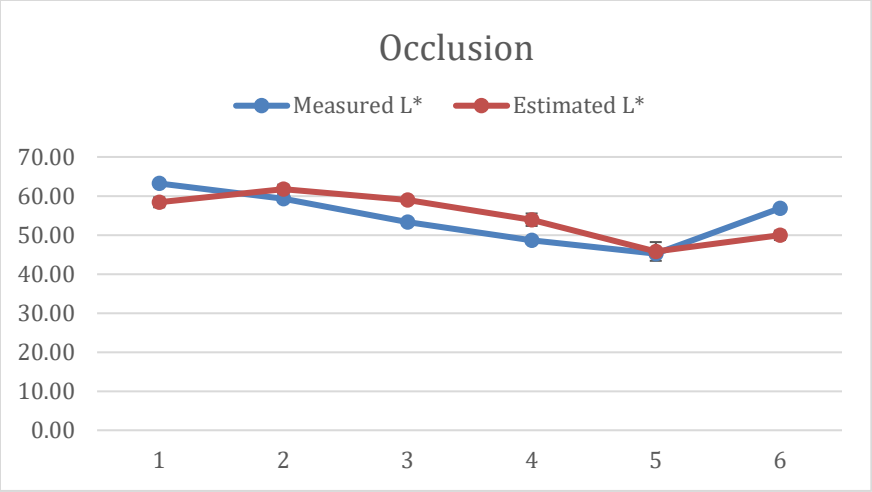

CIELAB L*

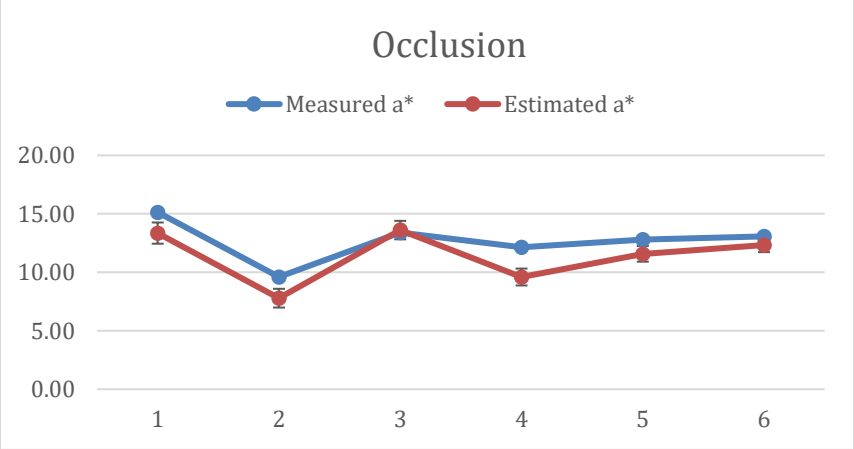

CIELAB a*

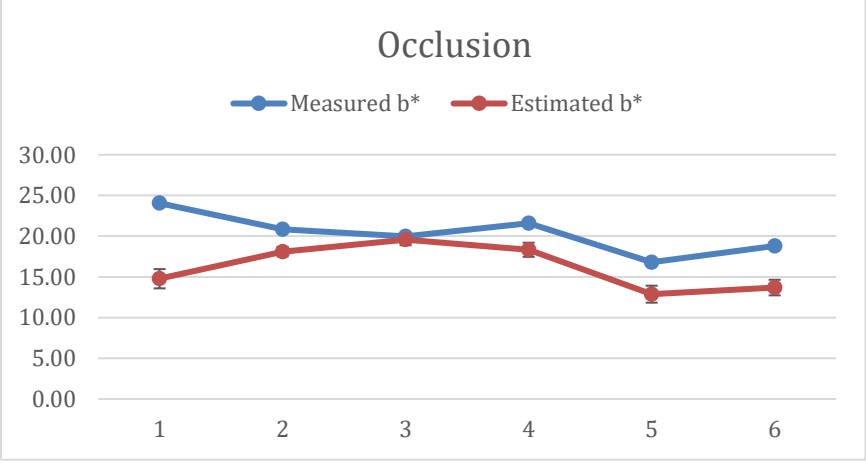

CIELAB b*

Figure 4-8: Mean+/-SD of CIELAB values. Difference between measured and estimated colorimetric data for each of 6 subjects at occlusion.

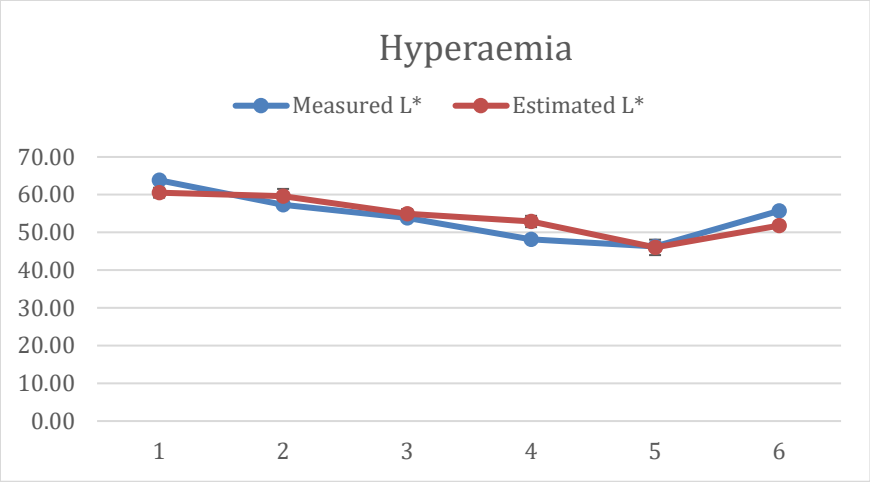

CIELAB L*

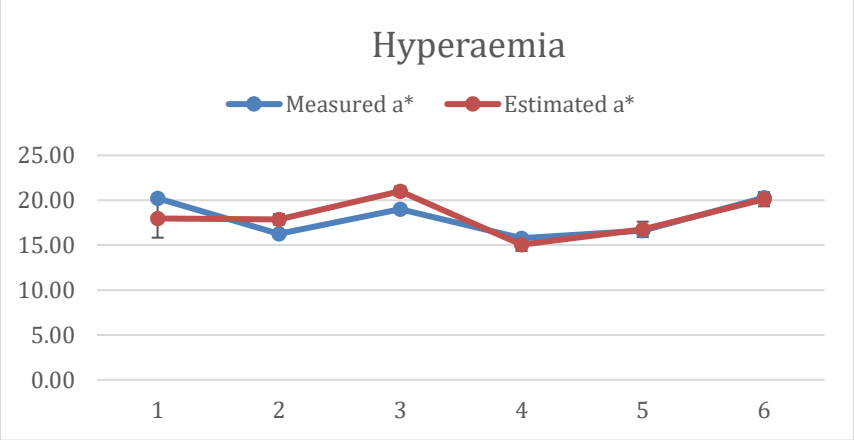

CIELAB a*

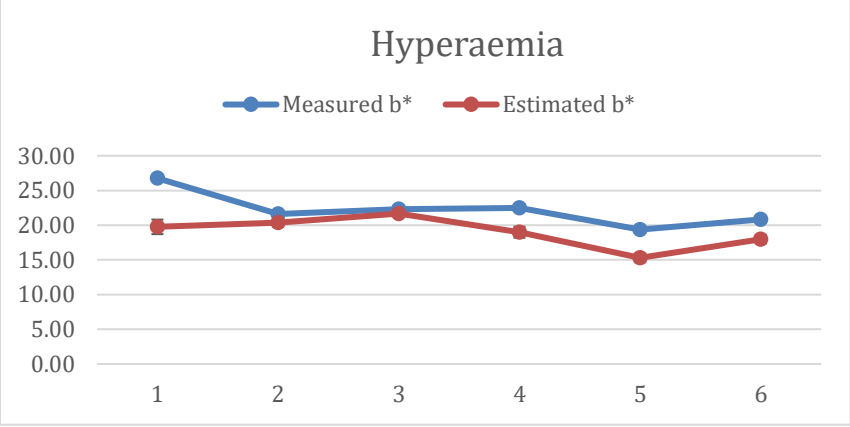

CIELAB b*

Figure 4-9: Mean+/-SD of CIELAB values. Difference between measured and estimated colorimetric data for each of 6 subjects at hyperaemia.

Table 4-2: CIELAB values for each subject's estimated versus measured colorimetric data during each physiological state.

	Subj	L*meas	L*est	a*meas	a*est	b*meas	b*est	Δ L*	Δ a*	Δ b*	Δ E*
Baseline	2.1	64.72	60.21	16.13	15.45	27.09	19.46	4.51	0.68	7.63	8.89
	2.2	60.79	60.53	10.44	17.96	22.10	19.76	0.26	7.52	2.35	7.88
	2.3	57.41	55.97	13.88	13.72	23.74	21.59	1.45	0.16	2.15	2.60
	2.4	49.83	52.57	13.18	12.74	23.27	16.98	2.74	0.44	6.29	6.87
	2.5	49.92	48.97	13.62	13.12	20.07	16.68	0.95	0.50	3.40	3.57
	2.6	59.93	55.08	13.63	13.49	21.98	18.49	4.84	0.14	3.49	5.97
	M	57.10	55.56	13.48	14.41	23.04	18.83	**2.46**	**1.57**	**4.22**	**5.13**
Occlusion	2.1	63.21	58.38	15.13	13.35	24.05	14.77	4.83	1.78	9.27	10.60
	2.2	59.32	61.75	9.60	7.79	20.84	18.10	2.43	1.82	2.73	4.08
	2.3	53.28	58.95	13.40	13.61	19.96	19.57	5.67	0.21	0.39	5.69
	2.4	48.67	53.93	12.15	9.59	21.60	18.33	5.26	2.55	3.26	6.69
	2.5	45.23	45.79	12.81	11.58	16.80	12.88	0.57	1.23	3.93	4.16
	2.6	56.81	49.93	13.07	12.32	18.81	13.69	6.88	0.76	5.12	8.61
	M	54.42	54.79	12.69	11.37	20.34	16.22	**4.27**	**1.39**	**4.12**	**6.09**
Hyperaemia	2.1	63.83	60.53	20.20	17.96	26.76	19.76	3.30	2.24	7.00	8.06
	2.2	57.32	59.60	16.25	17.88	21.62	20.36	2.28	1.62	1.26	3.07
	2.3	53.84	54.93	19.01	21.01	22.29	21.67	1.09	2.00	0.62	2.36
	2.4	48.19	52.89	15.78	15.06	22.47	18.99	4.70	0.72	3.48	5.89
	2.5	46.28	46.03	16.62	16.76	19.37	15.30	0.25	0.14	4.07	4.08
	2.6	55.68	51.84	20.29	20.11	20.84	17.99	3.84	0.18	2.85	4.79
	M	54.19	54.30	18.03	18.13	22.22	19.01	**2.58**	**1.15**	**3.21**	**4.28**
							M	**3.10**	**1.37**	**3.85**	**5.13**

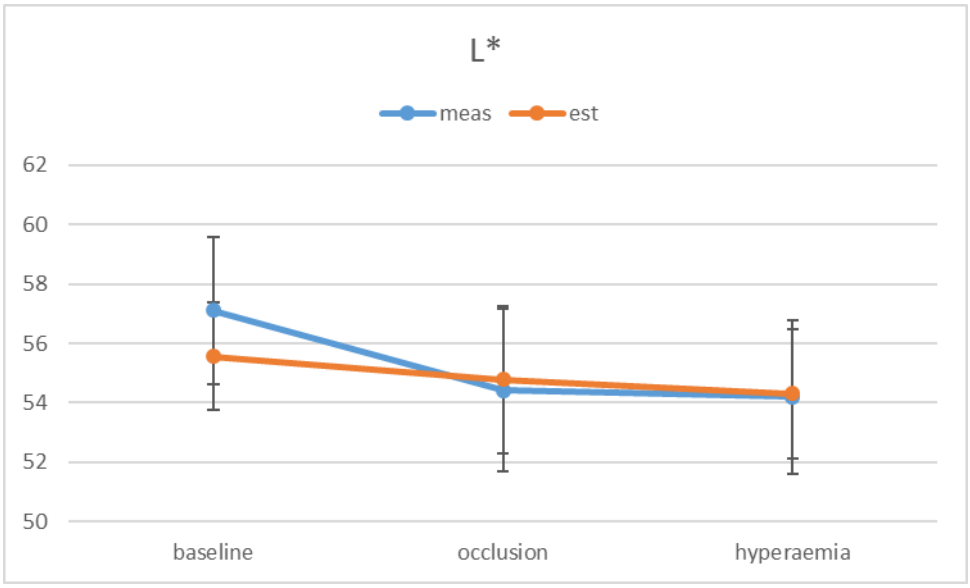

For both measured and estimated data, skin lightness (L*) slightly decreases over the physiological states, although this difference does not exceed the bounds of the mean standard error.

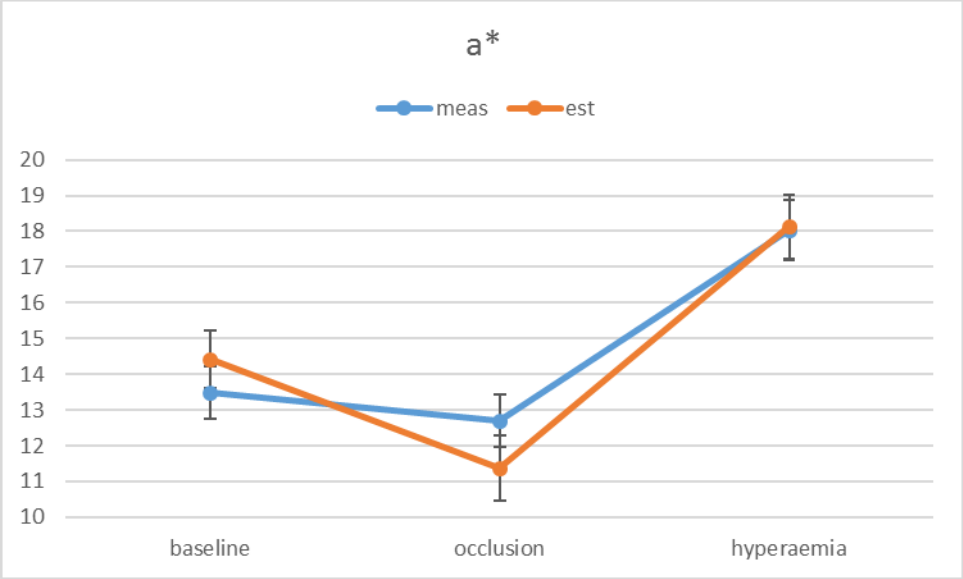

For both measured and estimated data, skin redness (a*) decreases from baseline to occlusion, and then increases from occlusion to hyperaemia.

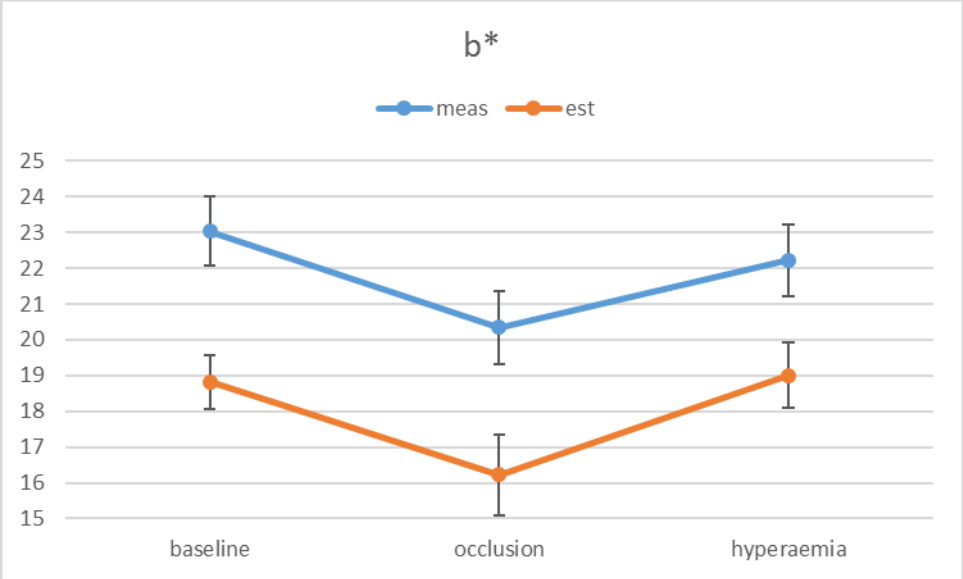

For both measured and estimated data, skin yellowness (b*) decreases from baseline to occlusion, and then increases from occlusion to hyperaemia.

Figure 4-10: Mean+/-SD of CIELAB values. Difference between measured and estimated colorimetric changes data across the 3 physiological states.

Table 4-3: Pairwise comparisons of measured vs. estimated changes in CIELAB values across physiological states.

		Meas ΔL*	Est ΔL*	ΔL* (error)	Meas Δa*	Est Δa*	Δa* (error)	Meas Δb*	Est Δb*	Δb* (error)
baseline	occlusion	2.68	0.77	**1.91**	0.79	3.04	**2.25**	2.7	2.61	**0.09**
	hyperaemia	2.91	1.26	**1.65**	4.55	3.72	**0.83**	0.82	0.18	**0.64**
occlusion	hyperamia	0.23	0.49	**0.26**	5.34	6.76	**1.42**	1.88	2.79	**0.91**
Mean				**1.27**			**1.50**			**0.55**

4.2.2. Discussion

The results revealed high consistency between the estimated and measured reflectance spectra. The curve shapes and absolute reflectance values show good fit at each physiological state (see Table 4-1; $RMSE_{baseline}$ = 0.012, $r_{baseline}$ > 0.99; $RMSE_{occlusion}$ = 0.004, $r_{occlusion}$ > 0.99 ; $RMSE_{hyperaemia}$ = 0.006, $r_{hyperaemia}$ > 0.99). The comparison between estimated and measured CIELAB L* values also showed a good (see Table 4-2; Δ L^*_{mean} = 3.10; Δ a^*_{mean} = 1.37; Δ b^*_{mean} = 3.85). Finally, the results showed that the estimated data were able to reliably predict changes in skin color across the three physiological states (see Table 4-3; MΔL^*_{error} = 1.27; MΔa^*_{error} = 1.50; MΔb^*_{error} = 0.55).

5. Summary, Conclusions, and Future Directions

The results from Experiment 1 showed non-trivial error in estimating spectral reflectance values for the individual subjects at rest. While the estimation of the curve shape, and chromatic estimation, was generally accurate, there was a noticeable scaling error in determining the absolute reflectance values (and subsequently in lightness values). It is likely the case that the primary source of error was in the use of a limited reference reflectance spectra set. The results from Experiment 2 (which employed a more specialized set of reference spectra) showed substantial

improvement in estimating reflectance and colorimetric values with high accuracy. These results support the notion that performance with spectral estimation methods is positively related to the similarity of the reference data to the test data (Li et al., 2003). Further, the results show that the ColourWorker method can reliably capture changes in skin color and reflectance that are due to changes in blood flow characteristic of physiological states.

Given the results of the current work, the ColourWorker methodology is a promising tool for investigating skin color and spectral reflectance changes over time, which can be used to extract physiological parameters such as melanin and hemoglobin properties. Future work should aim to incorporate more comprehensive reference spectra databases in order to improve the results. Future work should additionally test whether the methodology has good performance in estimating changes in skin reflectance when the physiological changes are more subtle and ecologically valid (e.g., during varying, naturally occurring, emotional states), rather than manipulated with a blood pressure cuff.

The accurate remote measurement of skin color and spectral reflectance is important due to its application across various fields, including medical, cosmetic, aesthetic, computational, and social science. Despite the obstacles inherent in extracting accurate colorimetric and spectral data from RGB cameras, the current work demonstrates that the ColourWorker method is able to estimate colorimetric and spectral reflectance values with good performance. The current work highlights the utility of skin color and spectral reflectance across several domains, the importance of developing computational methods to extract this information from inexpensive and non-invasive instruments, and the viability of this specific method to accurately estimate such data.

6. References

(Anderson et al., 2015)
Anderson, J. C., Hallam, M.-J., Nduka, C., & Osorio, D. (2015). The challenge of objective scar colour assessment in a clinical setting: using digital photography. *Journal of Wound Care*, *24*(8), 379–87.

(Berns, 2000)
Berns, R. S. (2000). *Billmeyer and Saltzman's principles of color technology*. New York: Wiley.

(Burriss et al., 2015)
Burriss, R. P., Troscianko, J., Lovell, P. G., Fulford, A. J. C., Stevens, M., Quigley, R., … Rowland, H. M. (2015). Changes in Women's Facial Skin Color over the Ovulatory Cycle are Not Detectable by the Human Visual System. *Plos One*,

(Changizi & Rio, 2010)
Changizi, M., & Rio, K. (2010). Harnessing color vision for visual oximetry in central cyanosis. *Medical Hypotheses*, *74*, 87–91.

(Changizi et al., 2006)
Changizi, M., Zhang, Q., & Shimojo, S. (2006). Bare skin, blood and the evolution of primate colour vision. *Biology Letters*, *2*(2), 217–21.

(Charkoudian et al., 1999)
Charkoudian, N., Stephens, D. P., Pirkle, K. C., Kosiba, W. A., & Johnson, J. M. (1999). Influence of female reproductive hormones on local thermal control of skin blood flow. *Journal of Applied Physiology*, *87*(5), 1719–1723.

(Chiao et al., 2000)
Chiao, C. C., Osorio, D., Vorobyev, M., & Cronin, T. W. (2000). Characterization of natural illuminants in forests and the use of digital video data to reconstruct illuminant spectra. *Journal of the Optical Society of America. A, Optics, Image Science, and Vision*, *17*(10), 1713–1721.

(Drummond, 1994)
Drummond, P. (1994). The effect of anger and pleasure on facial blood flow. *Australian Journal of Psychology*, *46*(2), 95–99.

(Gegenfurtner & Kiper, 2003)
Gegenfurtner, K. R., & Kiper, D. C. (2003). Color Vision. Annual Review of Neuroscience, 26, 181-206

(Goldstein et al., 2004)
Goldstein, E. B., Humphreys, G. W., Shiffrar, M., & Yost, W. A. (2004). Blackwell handbook of sensation and perception. John Wiley & Sons.

(Hsu, 2002)
Hsu, R. (2002). Face detection in color images. *IEEE Transactions on Pattern Analysis and Machine Intelligence*, *24*(5), 1–23. http://doi.org/10.1109/34.1000242

(Imai & Berns, 1999)
Imai, F. H., & Berns, R. S. (1999). Spectral estimation using trichromatic digital cameras. *Proceedings of the International Symposium on Multispectral Imaging and Color Reproduction for Digital Archives*, *42*, 42–49.

(Johnson, 1998)
Johnson, J. M. (1998). Physical training and the control of skin blood flow. *Medicine and Science in Sports and Exercise*, *30*(3), 382–386.

(Kikuchi et al., 2013)
Kikuchi, Masuda, & Hirao (2013). Imaging of hemoglobin oxygen saturation ratio in the face by spectral camera and its application to evaluate dark circles. *Skin Research and Technology*, 19(4), 499–507.

(Li et al., 2003)
Li, C., Cui, G., & Luo, M. R. (2003). The accuracy of polynomial models for characterising digital cameras. *Proc. AIC Interim. Meet*, 166-170.

(Nishidate et al., 2004)
Nishidate, I., Aizu, Y., & Mishina, H. (2004). Estimation of melanin and hemoglobin in skin tissue using multiple regression analysis aided by Monte Carlo simulation. *Journal of Biomedical Optics*, *9*(4), 700–710.

(Piérard, 1998)
Piérard, G. . E. (1998). EEMCO guidance for the assessment of skin colour. *Journal of the European Academy of Dermatology and Venereology : JEADV*, *10*(1), 1–11.

(Re et al., 2011)
Re, D. E., Whitehead, R. D., Xiao, D., & Perrett, D. I. (2011). Oxygenated-blood colour change thresholds for perceived facial redness, health, and attractiveness. *PloS One*, *6*(3), e17859.

(Stephen et al., 2009)
Stephen, I. D., Law Smith, M. J., Stirrat, M. R., & Perrett, D. I. (2009). Facial Skin Coloration Affects Perceived Health of Human Faces. *International Journal of Primatology*, *30*(6), 845–857.

(Stephen et al., 2012)
Stephen, I. D., Oldham, F. H., Perrett, D. I., & Barton, R. a. (2012). Redness Enhances Perceived Aggression, Dominance and Attractiveness in Men's Faces. *Evolutionary Psychology*, *10*(3), 562–572.

(Sun & Fairchild, 2002)
Sun, Q., & Fairchild, M. D. (2002). Statistical Characterization of Face Spectral Reflectances and Its Application to Human Portraiture Spectral Estimation. *Journal of Imaging Science and Technology*, *46*(6), 498–506.

(Yip & Sinha, 2002)
Yip, A. W., & Sinha, P. (2002). Contribution of color to face recognition. *Perception*, *31*(8), 995–1003.

(Young et al., 2016)
Young, S. G., Thorstenson, C. A., & Pazda, A. D. (2016). Facial redness, expression, and masculinity influence perceptions of anger and health. *Cognition and Emotion*, 1-12.

(Zhang et al., 2017)
Zhang, X., Wang, Q., Li, J., Zhou, X., Yang, Y., & Xu, H. (2017). Estimating spectral reflectance from camera responses based on CIE *XYZ* tristimulus values under multi-illuminants. *Color Research & Application*, *42*(1), 68–77.

(Zonios et al., 2001)
Zonios, G., Bykowski, J., & Kollias, N. (2001). Skin melanin, hemoglobin, and light scattering properties can be quantitatively assessed in vivo using diffuse reflectance spectroscopy. *Journal of Investigative Dermatology*, *117*, 1452–1457.